EUROPEAN ORGANISATION FOR NUCLEAR RESEARCH

CERN-PPE/91-81
May 24, 1991

A Measurement of the Electroweak Couplings of Up and Down Type Quarks Using Final State Photons in Hadronic Z^0 Decays

The OPAL Collaboration

Abstract

The production rate of final state photons in hadronic Z^0 decays is measured as a function of $y_{cut} = M_{ij}^2/E_{cm}^2$, the jet resolution parameter and minimum mass of the photon-jet system. Good agreement with the theoretical expectation from an $O(\alpha\alpha_s)$ matrix element calculation is observed. Comparing the measurement and the prediction for y_{cut}=0.06, where the experimental systematic and statistical errors and the theoretical uncertainties are small, and combining this measurement with our result for the hadronic width of the Z^0, we derive partial widths of up and down type quarks to be

$$\Gamma_u = 333 \pm 55 \pm 72 \text{ MeV} \quad \text{and} \quad \Gamma_d = 358 \pm 37 \pm 48 \text{ MeV}$$

in agreement with the Standard Model expectations. We compare our yield with the QCD shower models including photon radiation. At low y_{cut} JETSET underestimates the photon yield, and ARIADNE describes the production rate well.

(To be submitted to Physics Letters B)

The OPAL Collaboration

G. Alexander[23], J. Allison[16], P.P. Allport[5], K.J. Anderson[9], S. Arcelli[2], J.C. Armitage[6], P. Ashton[16], A. Astbury[a], D. Axen[b], G. Azuelos[18,c], G.A. Bahan[16], J.T.M. Baines[16], A.H. Ball[17], J. Banks[16], G.J. Barker[13], R.J. Barlow[16], J.R. Batley[5], G. Beaudoin[18], A. Beck[23], J. Becker[10], T. Behnke[8], K.W. Bell[20], G. Bella[23], S. Bethke[11], O. Biebel[3], U. Binder[10], I.J. Bloodworth[1], P. Bock[11], H.M. Bosch[11], S. Bougerolle[b], B.B. Brabson[12], H. Breuker[8], R.M. Brown[20], R. Brun[8], A. Buijs[8], H.J. Burckhart[8], P. Capiluppi[2], R.K. Carnegie[6], A.A. Carter[13], J.R. Carter[5], C.Y. Chang[17], D.G. Charlton[8], J.T.M. Chrin[16], P.E.L. Clarke[25], I. Cohen[23], W.J. Collins[5], J.E. Conboy[15], M. Cooper[22], M. Couch[1], M. Coupland[14], M. Cuffiani[2], S. Dado[22], G.M. Dallavalle[2], S. De Jong[8], P. Debu[21], M.M. Deninno[2], A. Dieckmann[11], M. Dittmar[4], M.S. Dixit[7], E. Duchovni[26], G. Duckeck[11], I.P. Duerdoth[16], D.J.P. Dumas[6], G. Eckerlin[11], P.A. Elcombe[5], P.G. Estabrooks[6], E. Etzion[23], F. Fabbri[2], M. Fincke-Keeler[a], H.M. Fischer[3], D.G. Fong[17], C. Fukunaga[24], A. Gaidot[21], O. Ganel[26], J.W. Gary[11], J. Gascon[18], R.F. McGowan[16], N.I. Geddes[20], C. Geich-Gimbel[3], S.W. Gensler[9], F.X. Gentit[21], G. Giacomelli[2], V. Gibson[5], W.R. Gibson[13], J.D. Gillies[20], J. Goldberg[22], M.J. Goodrick[5], W. Gorn[4], C. Grandi[2], E. Gross[26], J. Hagemann[8], G.G. Hanson[12], M. Hansroul[8], C.K. Hargrove[7], P.F. Harrison[13], J. Hart[5], P.M. Hattersley[1], M. Hauschild[8], C.M. Hawkes[8], E. Heflin[4], R.J. Hemingway[6], R.D. Heuer[8], J.C. Hill[5], S.J. Hillier[1], D.A. Hinshaw[18], C. Ho[4], J.D. Hobbs[9], P.R. Hobson[25], D. Hochman[26], B. Holl[8], R.J. Homer[1], S.R. Hou[17], C.P. Howarth[15], R.E. Hughes-Jones[16], R. Humbert[10], P. Igo-Kemenes[11], H. Ihssen[11], D.C. Imrie[25], L. Janissen[6], A. Jawahery[17], P.W. Jeffreys[20], H. Jeremie[18], M. Jimack[2], M. Jobes[1], R.W.L. Jones[13], P. Jovanovic[1], D. Karlen[6], K. Kawagoe[24], T. Kawamoto[24], R.K. Keeler[a], R.G. Kellogg[17], B.W. Kennedy[15], C. Kleinwort[8], D.E. Klem[19], T. Kobayashi[24], T.P. Kokott[3], S. Komamiya[24], L. Köpke[8], R. Kowalewski[6], H. Kreutzmann[3], J. von Krogh[11], J. Kroll[9], M. Kuwano[24], P. Kyberd[13], G.D. Lafferty[16], F. Lamarche[18], W.J. Larson[4], J.G. Layter[4], P. Le Du[21], P. Leblanc[18], A.M. Lee[17], M.H. Lehto[15], D. Lellouch[8], P. Lennert[11], C. Leroy[18], L. Lessard[18], S. Levegrün[3], L. Levinson[26], S.L. Lloyd[13], F.K. Loebinger[16], J.M. Lorah[17], B. Lorazo[18], M.J. Losty[7], X.C. Lou[12], J. Ludwig[10], M. Mannelli[8], S. Marcellini[2], G. Maringer[3], A.J. Martin[13], J.P. Martin[18], T. Mashimo[24], P. Mättig[3], U. Maur[3], T.J. McMahon[1], J.R. McNutt[25], F. Meijers[8], D. Menszner[11], F.S. Merritt[9], H. Mes[7], A. Michelini[8], R.P. Middleton[20], G. Mikenberg[26], J. Mildenberger[6], D.J. Miller[15], C. Milstene[23], R. Mir[12], W. Mohr[10], C. Moisan[18], A. Montanari[2], T. Mori[24], M.W. Moss[16], T. Mouthuy[12], P.G. Murphy[16], B. Nellen[3], H.H. Nguyen[9], M. Nozaki[24], S.W. O'Neale[8,d], B.P. O'Neill[4], F.G. Oakham[7], F. Odorici[2], M. Ogg[6], H.O. Ogren[12], H. Oh[4], C.J. Oram[e], M.J. Oreglia[9], S. Orito[24], J.P. Pansart[21], B. Panzer-Steindel[8], P. Paschievici[26], G.N. Patrick[20], S.J. Pawley[16], P. Pfister[10], J.E. Pilcher[9], J.L. Pinfold[26],

D.E. Plane[8], P. Poffenberger[a], B. Poli[2], A. Pouladdej[6], E. Prebys[8], T.W. Pritchard[13], H. Przysiezniak[18], G. Quast[8], M.W. Redmond[9], D.L. Rees[1], K. Riles[4], S.A. Robins[13], D. Robinson[8], A. Rollnik[3], J.M. Roney[9], S. Rossberg[10], A.M. Rossi[2,f], P. Routenburg[6], K. Runge[10], O. Runolfsson[8], D.R. Rust[12], S. Sanghera[6], M. Sasaki[24], A.D. Schaile[10], O. Schaile[10], W. Schappert[6], P. Scharff-Hansen[8], P. Schenk[a], H. von der Schmitt[11], S. Schreiber[3], J. Schwarz[10], W.G. Scott[20], M. Settles[12], B.C. Shen[4], P. Sherwood[15], R. Shypit[b], A. Simon[3], P. Singh[13], G.P. Siroli[2], A. Skuja[17], A.M. Smith[8], T.J. Smith[8], G.A. Snow[17], R. Sobie[g], R.W. Springer[17], M. Sproston[20], K. Stephens[16], H.E. Stier[10], D. Strom[9], H. Takeda[24], T. Takeshita[24], P. Taras[18], S. Tarem[26], P. Teixeira-Dias[11], N.J. Thackray[1], T. Tsukamoto[24], M.F. Turner[5], G. Tysarczyk-Niemeyer[11], D. Van den plas[18], R. Van Kooten[8], G.J. VanDalen[4], G. Vasseur[21], C.J. Virtue[19], A. Wagner[11], C. Wahl[10], J.P. Walker[1], C.P. Ward[5], D.R. Ward[5], P.M. Watkins[1], A.T. Watson[1], N.K. Watson[8], M. Weber[11], S. Weisz[8], P.S. Wells[8], N. Wermes[11], M. Weymann[8], M.A. Whalley[1], G.W. Wilson[21], J.A. Wilson[1], I. Wingerter[8], V-H. Winterer[10], N.C. Wood[16], S. Wotton[8], T.R. Wyatt[16], R. Yaari[26], Y. Yang[4,h], G. Yekutieli[26], I. Zacharov[8], W. Zeuner[8], G.T. Zorn[17].

[1]School of Physics and Space Research, University of Birmingham, Birmingham, B15 2TT, UK
[2]Dipartimento di Fisica dell' Università di Bologna and INFN, Bologna, 40126, Italy
[3]Physikalisches Institut, Universität Bonn, D-5300 Bonn 1, FRG
[4]Department of Physics, University of California, Riverside, CA 92521 USA
[5]Cavendish Laboratory, Cambridge, CB3 0HE, UK
[6]Carleton University, Dept of Physics, Colonel By Drive, Ottawa, Ontario K1S 5B6, Canada
[7]Centre for Research in Particle Physics, Carleton University, Ottawa, Ontario K1S 5B6, Canada
[8]CERN, European Organisation for Particle Physics, 1211 Geneva 23, Switzerland
[9]Enrico Fermi Institute and Department of Physics, University of Chicago, Chicago Illinois 60637, USA
[10]Fakultät für Physik, Albert Ludwigs Universität, D-7800 Freiburg, FRG
[11]Physikalisches Institut, Universität Heidelberg, Heidelberg, FRG
[12]Indiana University, Dept of Physics, Swain Hall West 117, Bloomington, Indiana 47405, USA
[13]Queen Mary and Westfield College, University of London, London, E1 4NS, UK
[14]Birkbeck College, London, WC1E 7HV, UK
[15]University College London, London, WC1E 6BT, UK
[16]Department of Physics, Schuster Laboratory, The University, Manchester, M13 9PL, UK

[17]Department of Physics and Astronomy, University of Maryland, College Park, Maryland 20742, USA
[18]Laboratoire de Physique Nucléaire, Université de Montréal, Montréal, Quebec, H3C 3J7, Canada
[19]National Research Council of Canada, Herzberg Institute of Astrophysics, Ottawa, Ontario K1A 0R6, Canada
[20]Rutherford Appleton Laboratory, Chilton, Didcot, Oxfordshire, OX11 0QX, UK
[21]DPhPE, CEN Saclay, F-91191 Gif-sur-Yvette, France
[22]Department of Physics, Technion-Israel Institute of Technology, Haifa 32000, Israel
[23]Department of Physics and Astronomy, Tel Aviv University, Tel Aviv 69978, Israel
[24]International Centre for Elementary Particle Physics and Dept of Physics, University of Tokyo, Tokyo 113, and Kobe University, Kobe 657, Japan
[25]Brunel University, Uxbridge, Middlesex, UB8 3PH UK
[26]Nuclear Physics Department, Weizmann Institute of Science, Rehovot, 76100, Israel

[a]University of Victoria, Dept of Physics, P O Box 3055, Victoria BC V8W 3P6, Canada
[b]University of British Columbia, Dept of Physics, 6224 Agriculture Road, Vancouver BC V6T 1Z1, Canada
[c]Also at TRIUMF, Vancouver, Canada V6T 2A3
[d]On leave from Birmingham University, Birmingham B15 2TT, UK
[e]Univ of Victoria, Dept of Physics, P.O. Box 1700, Victoria BC V8W 2Y2, Canada and TRIUMF, Vancouver, Canada V6T 2A3
[f]Present address: Dipartimento di Fisica, Università della Calabria and INFN, 87036 Rende, Italy
[g]University of British Columbia, Dept of Physics, 6224 Agriculture Road, Vancouver BC V6T 2A6, Canada and IPP, McGill University, High Energy Physics Department, 3600 University Str, Montreal, Quebec H3A 2T8, Canada
[h]On leave from Research Institute for Computer Peripherals, Hangzhou, China

1 Introduction

In this letter we present an analysis of final state photons emitted from quarks [1] in multihadronic decays of the Z^0. As discussed in detail in [2], the final state radiation provides a way of disentangling the weak couplings of up and down type quarks. Briefly, it exploits the fact that photons couple to the square of the charge of the emitting fermion. As a result up type quarks are enriched in a theoretically known ratio in events with a hard photon relative to the overall multihadron sample. The observed cross sections allow one to infer the weak couplings.

An almost background-free signal of about 250 final state photons is observed. After correcting the photon yield for detector effects and experimental cuts we compare it to a matrix element calculation in $O(\alpha\alpha_s)$ of Kramer and Lampe [3] as well as to the QCD shower programs JETSET [4] and ARIADNE [5], which both include the generation of final state photons.

A first measurement exploiting this method, based on about 27,000 multihadronic Z^0 decays, can be found in [6]. The current analysis is based on a sixfold increase of data, together with smaller systematic uncertainties and an improved theoretical calculation of the final state photon rate.

2 The OPAL Detector

This analysis is based on an integrated luminosity of about 6.6 pb^{-1} collected with the OPAL detector [7] at LEP. The data were recorded at center-of-mass energies E_{cm} between 88.28 and 94.28 GeV around the Z^0 pole.

The most important components of OPAL for this study are the main central drift chamber and the barrel part of the electromagnetic calorimeter. The central detector provides a measurement of the momenta of charged particles over almost the entire solid angle in a magnetic field of 0.435 T. The electromagnetic calorimeter covers the solid angle up to $|\cos\theta| \leq 0.98$, where θ is the polar angle with respect to the beam direction. Its barrel part ($|\cos\theta| \leq 0.82$) is used for the photon identification in this analysis and consists of 9440 lead-glass blocks of 24.6 radiation lengths, pointing towards the interaction region and each subtending an angular region of approximately 40x40 mrad^2. The presampler for electromagnetic showers and the hadron calorimeter served as cross checks for the photon identification. The presampler is located between the coil and the lead glass calorimeter. It consists of a set of 16 double-planed chambers containing streamer-tubes with both wire and cathode-strip readout. The hadron calorimeter, consisting of nine planes of streamer-tube chambers within the iron return yoke of the magnet, is located directly behind the electromagnetic calorimeter. In addition to measuring hadron energies, it provides information on longitudinal shower development.

3 Selection of Events with Final State Photons

Multihadronic events are required to have at least five well measured tracks and more than seven clusters in the electromagnetic calorimeter. An accepted track, reconstructed from at least 20 hits in the main drift chamber, must have a minimum momentum transverse to the beam direction of 250 MeV, a reconstructed distance of closest approach to the beam axis of less than 5 cm, and a longitudinal displacement along the beam direction from the nominal interaction point of less than 30 cm at the point of closest approach to the beam. A cluster in the lead-glass calorimeter consists of at least one block and a total energy of more than 100 MeV in the barrel region ($|\cos\theta| < 0.82$) and of at least two adjacent blocks with a minimum total energy of 200 MeV in the endcap region ($0.82 < |\cos\theta| < 0.98$). The energy sum of all accepted clusters ΣE_{clu} must exceed $0.11 \cdot E_{cm}$. The energy deposition must be balanced along the beam direction so that $|\Sigma(E_{clu} \cdot \cos\theta)|/E_{cm} < 0.65$. These requirements were satisfied by 145,095 events. The acceptance for multihadronic events is estimated to be 0.975 with a systematic uncertainty of 0.010 and a fraction of background from τ pairs, and two-photon processes of less than 0.003 [8]. To select events with energetic, isolated photons we impose requirements on both the event topology and on the response of the electromagnetic calorimeter, requirements that largely eliminate the background due to neutral hadrons.

The multihadronic events are searched for isolated photon candidates of more than 7.5 GeV energy within a fiducial region of $|\cos\theta| \leq 0.72$. The latter cut is chosen to minimize the material in front of the lead glass and to retain a good discrimination power against π^0 background. No tracks and no other electromagnetic clusters were allowed within a cone of half-angle 15 degrees centered at the photon direction.

To ensure an isolation of the photon with respect to the jets, a minimum mass between the photon candidate and the jets were required. The jets were defined according to [9], requiring that the minimum scaled pair mass y_{ij},

$$y_{ij} = \frac{M_{ij}^2}{E_{vis}^2} \tag{1}$$

be smaller than a specified y_{cut}. The same definition for jets is used in theoretical calculations. In the jetfinder $M_{ij}^2 = 2 \cdot E_i \cdot E_j \cdot (1 - \cos\alpha_{ij})$, $E_{i,j}$ being the energies of jets i,j or the photon, α_{ij} their opening angle, and $E_{vis} = \Sigma E_{had} + E_\gamma$ the visible energy. The hadronic energy ΣE_{had} was calculated from the momentum of the charged tracks and from the energies of the clusters in the electromagnetic calorimeter. The following procedure was adopted to select events for various values of y_{cut} between 0.005 and 0.2.

- in a first step the photon is excluded from the event, and the particles and

clusters are grouped into jets according to some value of y_{cut}. The photon energy is included in E_{vis}.

- in a second step the photon is combined with all jets to find the combination with the minimum pair mass $y_{\gamma,jet}$. Events are retained if $\mathrm{Min}(y_{\gamma,jet}) > y_{cut}$ with the same value used to define jets. While the photon energy is, in general, precisely reconstructed, a potential bias on $y_{\gamma,jet}$ is due to double counting of the energy of the charged particles in the tracking chamber and the lead glass calorimeter. We correct for those using the method described in [10]. In addition we correct globally for the energies of undetected neutrinos and of neutral hadrons that do not deposit their full energy in the lead glass calorimeter:

$$\Sigma E_{had} \;=\; c \cdot (\Sigma E_{had})_{measured} \tag{2}$$

where c was empirically determined from well contained multihadronic events to be
$c = 1.14$ to yield $< \Sigma E_{had} > = \; E_{cm}$.

After these cuts we retain 339 events for $y_{cut} = 0.005$.

Background to direct photons stems from neutral hadrons and particularly from photons due to π^0 decays. It is suppressed further by requiring the properties of the electromagnetic cluster to be consistent with that expected from a single photon. In a first step clusters were selected that consist of no more than 15 lead-glass blocks and have a width, defined by

$$W = \sqrt{\frac{\Sigma E_i \cdot ((\phi_i - < \phi >)^2 + (\theta_i - < \theta >)^2)}{\Sigma E_i}}, \tag{3}$$

of less than 30 mrad. Here ϕ_i and θ_i are the polar and azimuthal angles of each block i in the cluster and E_i is the energy deposited in the block. $< \phi >$ and $< \theta >$ describe the centroid of the cluster, and the summation runs over all blocks in the cluster. The corresponding distributions of the photon candidates are displayed in figures 1a,b for y_{cut}=0.005.

The final requirement is that sharing of energy among the blocks must be consistent with that expected from a photon. For this purpose a cluster shape variable

$$C = \frac{1}{N_{block}} \sum \frac{(E_i^{exp} - E_i^{obs})^2}{\sigma_i^2} \tag{4}$$

is calculated for each cluster, where E_i^{exp}, σ_i and E_i^{obs} denote the expected energy, its variation and the observed energy of block i, respectively. The summation is over all blocks of the cluster. C is then required to be less than 1.5. The distributions in C of the isolated clusters before the cuts on the cluster properties

y_{cut}	cand.	N_{had}	N_{ISR}	N_{FSR}	Acceptance	$N_{FSR}^{corr.}$
0.005	276	9.5±4.5	13.3±1.3	253.2±17.3	0.286±0.009	885.5±60.5
0.010	262	8.5±4.1	13.2±1.3	240.3±16.7	0.338±0.010	710.5±49.4
0.020	233	5.5±2.7	12.6±1.3	214.9±15.6	0.395±0.012	543.8±39.5
0.040	181	4.5±2.0	11.3±1.1	165.6±13.6	0.491±0.018	335.9± 27.6
0.060	149	1.8±1.5	10.1±1.0	137.1±12.3	0.532±0.023	257.7±23.1
0.080	118	2.1±1.1	7.9±0.8	108.0±10.9	0.566±0.028	190.7±19.3
0.100	97	2.3±1.2	6.1±0.6	88.6±9.9	0.570±0.030	155.4± 17.4
0.120	79	2.3±1.2	4.6±1.5	72.1±9.1	0.547±0.031	131.8± 16.6
0.140	71	2.4±1.3	4.1±1.2	64.5±8.6	0.541±0.033	119.2±15.9
0.160	63	2.2±1.2	3.4±1.0	57.4±8.1	0.553±0.036	103.8±14.7
0.180	59	2.5±1.4	3.2±1.0	53.3±7.9	0.547± 0.037	97.4±14.4
0.200	59	2.6±1.4	2.8±1.0	53.6±7.9	0.532± 0.038	100.8±14.8

Table 1: Background contribution and acceptance. The observed yield of photon candidates (cand.), the background contributions, the acceptance and the corrected number of events with final state photons (N_{FSR}^{corr}) are listed. Background from hadrons (N_{had}) and from initial state radiation (N_{ISR}) is considerd. The error on the acceptance is only statistical.

are displayed in figures 2a-c for the three energy intervals 7.5< E_{clu} <15, 15< E_{clu} <25, and E_{clu} >25 GeV with y_{cut}=0.005.

The numbers of observed events as a function of y_{cut} are listed in table 1. For y_{cut}=0.005 these cuts leave 276 photon candidates in the sample.

4 Efficiency and Background Contributions to the Photon Sample

The efficiency of the photon selection is determined from a sample of unambiguous photons in radiative lepton-pair and in $e^+e^- \to \gamma\gamma$ [11] events recorded during the same running period. This reference sample consists of 210 photons. The efficiency for photon identification is 89.8±2.7% and includes losses due to conversions before and inside the chamber (5.7±2.2%) and due to the requirements on the cluster shape (5.0±1.6%). The cluster shapes observed in these events are also shown in figures 2a-c and are seen to agree very well with the photon candidates in the multihadronic events. Also shown are results of the simulation of photons which reproduce well the observed spectrum of the reference sample.

In the following the remaining background from narrow neutral jets in the observed candidate events, surviving the cuts described above, will be considered.

The contamination is estimated by several independent methods. By assuming isospin symmetry, the background estimate used in this analysis is obtained from the number of narrow *charged* jets. Cross checks are performed by using the different distributions in C of genuine photons, of π^0's and of other hadronic contributions to the isolated clusters and by studying the response in the hadron calorimeter and the barrel presampler. These cross checks yield results consistent with the estimates given below.

Multihadronic Z^0 decays as generated with the models of [4] and [12], interfaced with a detailed simulation of the OPAL detector, serve as a tool for understanding which kind of fragmentation background might contribute to the selected sample. Within about 200,000 generated events only π^0's are found to produce isolated clusters surviving all requirements. We also find that other particles can produce isolated clusters that may resemble those of genuine photons, although they are in most cases much broader. These particles include K^0_L's, neutrons, and decays of high momentum particles like η or $K^{*0} \rightarrow K^0\pi^0$, yielding overlapping showers in the lead glass calorimeter. These backgrounds were studied with dedicated single particle Monte Carlo samples. The Monte Carlo studies provided guidance but the background is determined from the data itself.

Two background contributions, single as well as unresolvable pairs of neutral particles, are estimated using charged particles. The same topological requirements used to select photon candidates are applied to the charged particles. This procedure has been applied for several values of y_{cut} between 0.005 and 0.2.

- For the first background source, π^0's and single neutral stable particles, single charged particles are considered. For $y_{cut} = 0.005$ (0.06), 44 (6) isolated tracks are retained. To ensure reliable measurement, strict criteria are applied, leading to a track finding efficiency of 0.93±0.01, obtained from muon and electron pair events. To translate the yield of isolated charged particles into the yield of isolated neutral clusters several corrections are applied. Isospin symmetry implies $n_{\pi^0}=1/2 \cdot n_{\pi^\pm}$, $n_{K^0_L}=1/2 \cdot n_{K^\pm}$, $n_{neutron}= n_p$, where at least the first two relations are experimentally supported (for a review see [14]). The efficiencies to reject π^0's using the cluster shape are determined with a detailed simulation of the OPAL detector to be 0.65, 0.40, and 0.20 in the respective energy intervals $7.5< E_{clu} <15$ GeV, $15< E_{clu} <25$ GeV, $E_{clu} >25$ GeV. The lead glass response to π^0's, obtained from a simulation, is shown in figures 2a-c. The corresponding efficiency to reject K^0_L's is found to be 0.986±0.005 and for neutrons to be, 0.993±0.005. Using in addition the relative fractions of pions, kaons, and protons for particle energies above 7.5 GeV, which are nearly independent of the center-of-mass energy [15], leads to an estimated background from single isolated neutral particles of 8.5±1.2 and 1.5±0.5 (statistical errors) events for y_{cut} of 0.005 and 0.06. Most of the isolated charged tracks have energies somewhat above 7.5 GeV.

Uncertainties in these corrections stem mainly from the measured ratio of neutral over charged pions, and from the $\pi^{\pm}$ fraction in the stable charged particle yield and are about 25% and 10%. A total systematic error of 50% will be assigned to this background source.

- As a second kind of hadronic background the overlap of two particles in one cluster is considered. Because of the many possible contributions and because of the lack of precise measurements of resonance production at large $x = 2 \cdot E_{had}/E_{cm}$ and of the rate of very narrow jets, the estimate is less certain. In a first step we study the conditions that lead this kind of background to produce electromagnetic clusters resembling those accepted as photon candidates. To this end we simulated 300-500 single decays each of $K^{*0} \rightarrow K^0_L\pi^0$ and $K^0_s \rightarrow \pi^0\pi^0$. Of those, we reject 98.6% and 84%. All retained particle combinations had a decay opening angle of less than 40 mrads. In a second step the background from overlapping neutral particles is estimated by searching for two *charged* particles within 40 mrads [1] which, when combined, satisfy the kinematic requirements imposed on the isolated photons. Apart from ten particle combinations consistent with e^+e^- - pairs from photon conversions, four to twelve isolated charged particle combinations were found depending on the y_{cut}. Invoking isospin symmetry, and applying corrections for experimental distortions and for the rejection efficiency of their neutral counter-parts due to the cluster shape, one estimates a background of up to one neutral cluster. To take into account the uncertainty in the precise nature of the two overlapping particles and in the experimental corrections, a systematic uncertainty of $\pm 100\%$ was assigned to this contribution.

Other hadronic background contributions not accounted for by the charged particle estimate are electromagnetic decays like $\eta \rightarrow \gamma\gamma$. From simulation studies it is found that for cluster energies between 10 and 50 GeV, 0.980 ± 0.006 of these decays are rejected. As a result these contributions in the selected isolated clusters are negligible. In total a background of 9.5 ± 4.5 (1.8 ± 1.5) is estimated from the analysis of charged particle jets for a y_{cut} of 0.005 (0.06). The background is listed for various y_{cut} in the third column of table 1.

Additional background to the final state photons is due to initial state photons. On the Z^0 peak these are strongly suppressed, but 26.9% of the data for this analysis were collected slightly off the peak. At these energies the fraction of initial state photons is significantly increased. Taking the energy dependence into account, the number of initial state photons as expected by using the Monte Carlo

[1] This requirement is imposed in the plane transverse to the beam direction only. To take into account the worse resolution along the beam direction, the total opening angle has to be smaller than 170 mrad.

generator of [16] combined with the JETSET model to simulate the hadronic event structure is 13.3±1.3 (10.1±1.0) for y_{cut} = 0.005, (0.06) and is listed in column 4 of table 1.

5 Correction Procedure

For comparison with theoretical calculations, we need the yield of final state photons with just the cut on y applied. We therefore correct our data for the topological cuts on the minimum energy and isolation, and also for biases from the fragmentation, and for detector effects using the JETSET and ARIADNE shower models and a detailed simulation of the OPAL detector [13].

We distinguish two kinds of corrections to the yield. The first correction (c_1) accounts for the fraction of events lost when changing the selection from just the y_{cut} applied to the final partons in the shower programs to a selection combining the y_{cut}, energy and isolation requirement after the partons have fragmented. For low values of y_{cut}, this correction can be substantial and depends on the proper description of photon radiation in the simulation in a kinematical region that cannot be tested experimentally. However, since $y \propto E_\gamma \cdot (1 - \cos\alpha)$ with α being the angle between the photon and the closest jet, this correction is less important for larger y_{cut}'s. The losses due to the energy and isolation cut are 52% for y_{cut}=0.005 and about 15% for y_{cut}=0.06. At the higher y_{cut}, the losses are almost completely due to the isolation cut. The second correction (c_2) is due to the detector performance alone. For small y_{cut} the correction c_2 is slightly increasing and saturates at $c_2 \sim 1.10$ for $y > 0.04$ and is mainly due to the isolation cone. An additional correction of 1.43 for the restricted angular range of accepted photons has to be applied.

In estimating the systematic uncertainties of these corrections we distinguish between two sources, the modelling of photon emission in multihadronic events and the simulation of the detector response. The various contributions to the systematic error are listed in table 2.

Since we cannot compare the photon yield predicted from the simulations at lower energies and smaller isolation cones with the data, we assign a systematic uncertainty $\delta c_1^{extr}(y_{cut})$ to the correction according to the following prescription: if $f(y_{cut})$ is the fraction of 'true' photons retained for a y_{cut} but having an energy smaller than 7.5 GeV or additional particles in the isolation cone, we assign $\frac{\delta c_1^{extr}}{c_1}(y_{cut}) = 0.25 \cdot f(y_{cut})$. This leads to a systematic uncertainty of 13% at y_{cut}=0.005 and 4.5% for $y_{cut} \geq$0.04. A way to estimate if the assigned uncertainty is appropriate is to compare the two Monte Carlo generators JETSET [4] and ARIADNE [5], which include final state photons. The correction factors c_1 agree within 5% although the absolute photon yields predicted by the two generators

y_{cut}	energy/isolation	photon identification	jet reconstruction
0.005	13.0	2.7	1.0
0.010	11.0	2.7	1.1
0.020	8.0	2.7	1.5
0.040	4.5	2.7	2.0
0.060	4.5	2.7	2.5
≥ 0.080	4.5	2.7	2.7

Table 2: Contributions to systematic uncertainties of corrections (%) Listed are the assigned contributions in percent to the systematic error of the yield of events with final state photon radiation. The contributions to c_1 come from the fraction of events lost due to the energy cut and the isolation criterium (column 2). The contributions to c_2 come from the photon identification (column 3) and from distortions in the measurement of the angle and direction of the jets (column 4).

differ by about 40%.

We further investigate the systematic uncertainty due to potential misrepresentations of the jet properties by smearing the reconstructed energies and directions and by rescaling the jet energies. From consistency checks between simulation and data we find that the energy and angular resolution of jets are well described by the Monte Carlo. Moreover, even if we change the energy resolution by an additional 15% of the jet energy, or the resolution of the direction by 15 degrees we find only a negligible effect on the final yield. However, we cannot exclude a systematic shift of the energy by $\pm 6\%$. Such a deviation leads to changes of up to $\pm 2.7\%$ which we account for in the systematic error. Its dependence on y_{cut} is listed in table 2.

6 The Cross Section of Final State Photon Radiation

Applying the corrections c_1 and c_2, we obtain the corrected numbers of events with final state photons listed in table 1. We convert these numbers into fraction of all multihadronic events as a function of y_{cut}. The results are listed in table 3 and are shown in figure 3.

The yield decreases by about a factor of ten for an increase of y_{cut} from 0.005 to 0.2. At these high y_{cut} values the photon and the jets are mostly in different hemispheres, and a further increase of y_{cut} has only a marginal effect on the fraction. It should be noted that the results for the various y_{cut}'s are correlated. The

uncertainty in c_1 at very low y_{cut} leads to a large systematic error which decreases rapidly with increasing y_{cut}. For $y_{cut} \geq 0.04$ the statistical error dominates.

In table 3 and figures 3a,c we also display the expectations from the $O(\alpha\alpha_s)$ calculation of Kramer and Lampe [3] and the two QCD shower models JETSET [4] and ARIADNE [5].

Kramer and Lampe have calculated the cross sections $\sigma_{\gamma+n\ jet}$ for $n \leq 3$ as a function of y_{cut} between 0.01 and 0.20. The calculation is basically the same as for the n-jet rates in overall multihadronic events [21] which has been used in QCD studies. Their result is expressed as

$$\sigma(Z^0 \rightarrow \gamma + \ jets)(y_{cut}) \propto \ \Sigma_{n=1}^{n=3} g_n(y_{cut}) \tag{5}$$

where the coefficients g_n describe the production rate of multihadronic events with n jets plus a photon. The values g_1 and g_3 are tree level results. The value g_2 for two jet events includes $O(\alpha_s)$ higher order QCD corrections, calculated as in [21]. The coefficients g_2 and g_3 depend explicitly on the strong coupling constant α_s. It should be noted that since the jet rates are only given in first order α_s, the result only depends on the *ratio* of $\Lambda_{\overline{MS}}$ and the renormalization scale $\mu^2 = f \cdot E_{cm}^2$. Therefore no explicit variation of the scale will be considered. Variations of α_s affect both the absolute yield and the jet multiplicity of events with final state photons, an effect that is taken into account in the systematic error. As discussed in [20] the calculation is close to the recombination scheme adopted in this analysis to define jets.

Both QCD shower models [4, 5] have been extensively tested using the overall multihadronic sample. They give a very good account of the overall event structure and the single particle distributions over a large range of c.m. energies. They are based, however on several assumptions and do not give rigorous predictions. For our comparison we adopt the default parametrizations with parameter values optimized in [17]. We can thus interpret the results for the final state photon bremsstrahlung as a new kind of test of the underlying model. A more detailed comparison will be presented in [18].

Uncertainties in the predictions of the matrix element calculation arise from the limited order of the QCD corrections considered, while uncertainties in the shower models come from the modelling of gluon and photon emission.

The uncertainty of the matrix element calculation is determined by the uncertainty of α_s. We base the estimate of this uncertainty on the results obtained from fits to the jet rates in the overall multihadronic events [19] and on the jet rates observed in the multihadronic events with final state photons. Using a theoretical calculation in $O(\alpha_s^2)$ yields $\alpha_s^{(2)}(M_{Z^0})=0.118\pm0.009$ for the jet rates. Since the theoretical calculation for the events with final state photons is only of $O(\alpha_s)$ this value is not directly applicable to the photon yield. Instead we fit the

overall observed jet rate with the first order part of the calculation [21] and find $\alpha_s^{(1)}$=0.177±0.013. Another determination of α_s uses the measured ratio of two jet events over the sum of two and three jet events in events with final state photons. We find ratios of 0.72±0.05 (y_{cut}=0.02) and 0.91±0.05 (y_{cut}=0.04), which correspond to $\alpha_s^{(1)}$=0.25±0.07. Since the cross sections for events with three jets plus a photon are only calculated at the tree level, this ratio is likely to yield too large an α_s. Based on these considerations we define the theoretical expectation conservatively to be the average of the theoretical predictions of the extreme cases (α_s=0.118 and α_s=0.25). We assign half of the difference as the theoretical uncertainty.

The procedure for defining events with final state photons used in the theoretical calculation is not identical to that used in the measurement, as described in section 3. Kramer and Lampe apply the y_{cut} algorithm to all partons *and* the photon. In addition their calculation of $O(\alpha_s)$ allows for at most three partons, while experimentally only hadrons can be measured. In the absence of a differential distribution for $q\bar{q}\gamma(g)$ we estimate how these differences change the cross section of final state photon events by using the model of an Abelian strong interaction as implemented in [4]. We exclude contributions from $q\bar{q}q\bar{q}$ and treat one of the gluons as a photon. We expect the topologies of the Abelian events should be very similar to those of $q\bar{q}\gamma(g)$ events. We find for $y_{cut} \leq$0.06 the yield of final state photon events to be reduced by less than 6%. But for large y_{cut} the reduction is large (38% for y_{cut}=0.2). The different procedures affect the two and three jet rates only marginally, whereas the difference in the one jet rate can be substantial: at y_{cut}=0.2 only 41.7% of the one jet events are retained with the procedure of Kramer and Lampe.

The predictions of the shower models are uncertain because of ambiguities in the parametrizations and the treatment of the kinematics of parton splitting. For this analysis we adopt the default parametrizations with parameters optimized to describe the overall event shape [17]. As the only uncertainty we consider the variation of the QCD scale parameter Λ (see discussion in [2]). Its possible variations are taken from fits to the three jet rate yielding ±30 MeV for both JETSET and ARIADNE.

For the comparison of the data with the shower models we neglect the error δc_1^{extr}, since these programs were used to determine the corrections. Within the limited statistical and systematic uncertainties of the data we draw the following conclusions on the validity of the various predictions (see figs. 3a-c).

- The matrix element calculation is in very good agreement with the data for $y_{cut} \leq 0.12$ but is one to two standard deviations below the data at high y_{cut} (figure 3a). Note that data at different values of y_{cut} are correlated. No prediction is given for y_{cut} <0.02 since the two jet rate is negative for α_s=0.25. As can be seen from figure 3b, at low y_{cut} <0.02, the three jet rate is large.

At y_{cut} >0.14 the one jet rate becomes prominent. Also shown in this figure are the expectations from the matrix element calculation. As can be seen, the theoretical two jet rate is in very good agreement with the measured rate for *all* y_{cut}. However, the theoretical calculation underestimates the one-jet rate significantly.

If we correct the yield according to the results of our analysis of the Abelian matrix element, a much better agreement between data and theory is found. As stated before, the change of the expected cross section is small for small y_{cut} $\leq$0.06 but significant for higher y_{cut}. Both for the total rate and for the individual jet rates the agreement between data and theory improves considerably, e.g. at y_{cut}=0.2 the expected photon yield increases from 0.28 to 0.45.

- JETSET underestimates the photon yield at very low y_{cut} by 30% with a significance of about three standard deviations. It agrees better for y_{cut} $\geq$0.06 with an expectation that is 10% lower at one standard deviation (figure 3c).

- ARIADNE reproduces the data well at low y_{cut} but tends to overestimate the measured yield for y_{cut} $\geq$0.04 by about 25%. The significance of this discrepancy is about one to two standard deviations (figure 3c).

7 The Electroweak Couplings of Up and Down Type Quarks

We use our measurement to determine the weak couplings of up and down type quarks. The method is discussed in detail in [2]. In brief, since final state photons couple to the square of the quark charge, the relative fractions of the quark species in multihadronic events with final state photons is different from those in the overall sample. The partial width of the Z^0 into a photon and jets is given by [3]

$$\Gamma(Z^0 \rightarrow \gamma + jets)(y_{cut}) \;=\; \frac{h}{9}\frac{\alpha}{2\pi}\Sigma g_i(y_{cut}) \cdot [3 \cdot c_d \;+\; 8 \cdot c_u] \qquad (6)$$

and the total hadronic width by

$$\Gamma(Z^0 \rightarrow q\bar{q}) \;=\; h \cdot (1 + \frac{\alpha_s}{\pi} + 1.42(\frac{\alpha_s}{\pi})^2) \cdot [3 \cdot c_d \;+\; 2 \cdot c_u] \qquad (7)$$

where

$$h = 3 \cdot \frac{G_F \cdot M_{Z^0}^3}{24 \cdot \pi\sqrt{2}} \qquad (8)$$

y_{cut}	$(N_{q\bar{q}\gamma}/N_{had}) \cdot 10^3$	ME	JETSET	ARIADNE
0.005	5.95±0.44±0.77		4.67±0.07	6.15±0.03
0.010	4.78±0.36±0.53		3.76±0.06	4.88±0.02
0.020	3.66±0.28±0.29	3.00±0.55	2.85±0.06	3.67±0.01
0.040	2.32±0.21±0.10	2.16±0.19	1.99±0.04	2.58±0.01
0.060	1.72±0.17±0.08	1.61±0.08	1.53±0.03	1.98±0.01
0.080	1.28±0.14±0.06	1.22±0.04	1.19±0.03	1.57±0.01
0.100	1.04±0.13±0.05	0.94±0.02	0.97±0.02	1.29±0.01
0.120	0.89±0.12±0.04	0.73±0.01	0.82±0.01	1.11
0.140	0.80±0.11±0.04	0.58±0.01	0.70±0.01	1.00
0.160	0.70±0.10±0.03	0.45±0.01	0.62±0.01	0.90
0.180	0.64±0.10±0.03	0.36	0.57±0.01	0.83
0.200	0.67±0.10±0.03	0.28	0.54±0.01	0.80

Table 3: Photon selection for various y_{cut}. The corrected fraction of events with final state photons over the total number of hadronic events is listed. The first error combines the statistical and systematic uncertainty of c_2, added in quadrature, the second is due to the energy and isolation cut. Also shown are the predictions from the matrix element calculation [3] (ME) and the parton shower Monte Carlos JETSET [4] and ARIADNE [5]. The error on the matrix element prediction reflects the uncertainty of α_s. The uncertainties assigned to the JETSET and ARIADNE predictions are only due to variations of the QCD scale parameter Λ. Note that the second error of the data is not relevant for the comparison of the JETSET and ARIADNE prediction to the data.

Here G_F is the Fermi coupling constant at the muon mass, M_Z the mass of the Z^0, α_s the strong and α the electromagnetic coupling constant. The

$$c_i \;=\; v_i^2 \;+\; a_i^2 \tag{9}$$

are the weak couplings of down and up type quarks to the Z^0, a_i and v_i denote the axial and vector couplings defined by

$$v_i \;=\; 2 \cdot I_{3,i}^L - 4 \cdot Q_i \cdot \sin^2\theta_{\rm W} \quad and \quad a_i^L \;=\; 2 \cdot I_{3,i} \tag{10}$$

with I_3^L, Q, and $\theta_{\rm W}$ the third weak isospin of the left component, the charge of the quarks and the weak mixing angle respectively. For formulae 7 and 8 we assumed the couplings of the various up, respectively down type quarks to be the same. This condition can be relaxed such that $3 \cdot c_d$ and $2 \cdot c_u$ can be replaced by the *sum* of the couplings of all up and down type quarks.

Adopting our measurements of the total hadronic Z^0 width and of the final state photon yield we can solve these two equations for the weak couplings c_d and c_u.

Since both JETSET and ARIADNE rely on model assumptions, we prefer to base our determination on the matrix element calculation of [3]. To minimize the systematic and statistical error we use y_{cut}=0.06. For this value the uncertainties from our energy and isolation cuts are small, and the statistical precision is adequate. Also, the theoretical uncertainties are small; variations of α_s contribute only a 5% uncertainty. For this y_{cut} almost 90% of the events are two jet events. The contributions from one and three jet events are only 7.3±1.6 % and 3.4±1.1 %. We thus avoid a large influence from the unknown higher order corrections for these rates and the different procedures to define the events with final state photons. The residual uncertainty was taken into account by assigning a systematic error to the theoretical calculation. It consists of a 6.1% uncertainty on the total cross section which is the difference of the two procedures using the Abelian matrix element, and a 2% error to take into account higher order corrections in the one jet cross section. This is 50% of the theoretical one jet contribution. Since both effects are expected to increase the theoretical expectation we add these uncertainties linearly, i.e. the final theoretical error will be ±8.1%. Using the measured values of Γ_{had} = 1739±17 MeV [8] and $(N_{q\bar{q}\gamma}/N_{had})$ = (1.72±0.17±0.08)·10^{-3} along with the prediction from the matrix element calculation $(N_{q\bar{q}\gamma}/N_{had})_{ME}$ = (1.61±0.15)·10^{-3}, which assumes standard model couplings, we find

$$3 \cdot c_d \;+\; 2 \cdot c_u \;=\; 6.75 \pm 0.02 \tag{11}$$

and

$$3 \cdot c_d \;+\; 8 \cdot c_u \;=\; 14.5 \pm 1.3 \pm 1.7 \tag{12}$$

as displayed in figure 4a. The first error is statistical, the second systematic. These two equations can be solved for the weak couplings of up and down type quarks separately. We find

$$c_u = 1.29 \pm 0.21 \pm 0.28 \quad (13)$$

$$c_d = 1.39 \pm 0.14 \pm 0.19 \quad (14)$$

As already indicated by the coincidence of the measured and expected photon yield, these values are in very good agreement with the standard model values of $c_d = 1.48$ and $c_u = 1.15$ for $\sin^2\theta_W = 0.23$. We can convert this measurement into branching fractions of up and down type quarks using $F_i = \frac{\Gamma_i}{\Gamma_{had}} = \frac{c_i}{\Sigma c_i}$, yielding

$$F_u = 0.191 \pm 0.031 \pm 0.040 \ , \quad F_d = 0.206 \pm 0.021 \pm 0.028 \quad (15)$$

or

$$\Gamma_u = 333 \pm 55 \pm 72 \ (MeV) \ , \quad \Gamma_d = 358 \pm 37 \pm 48 \ (MeV) \quad (16)$$

In fig.4b we display the one standard deviation contour for the correlation of Γ_u and Γ_d. Since $\delta\Gamma_{had}/\Gamma_{had}$ is much smaller than $\delta N_{q\bar{q}\gamma}/N_{q\bar{q}\gamma}$, the ellipse appears as a diagonal bar. Also indicated is the standard model value which is in good agreement with our measured values.

8 Summary and Discussion

We have compared our yield of final state photons in multihadronic events with the theoretical predictions from an $O(\alpha\alpha_s)$ matrix element calculation and the parton shower models JETSET and ARIADNE. We find good agreement with the matrix element prediction. A difference in the one jet rate seems to be due to the different procedures of defining final state photon events in the theoretical calculation and the experiment. There are indications that JETSET underestimates the photon yield at low y_{cut}, whereas ARIADNE reproduces the measurement well in general.

We use our measurement to determine the partial widths of up and down type quarks. Our values of 333±91 MeV and 358±61 MeV are in in good agreement with the standard model expectations of 296 and 382 MeV with uncertainties of about ±4 MeV depending on the top and the Higgs mass. Our measurement is also in very good agreement with the values obtained from combining the results obtained by the LEP experiments for individually identified bottom [26, 22, 23], and charm quarks [22, 23, 24, 25] yielding $\Gamma_b = 369 \pm 31$ MeV and $\Gamma_c = 322 \pm 53$ MeV. Errors in the measurements due to uncertainties in decay branching ratios have been treated as common errors in obtaining a LEP average. They contribute the major part of the final uncertainties. As pointed out in [2], the errors from the

measurement using final state photons are almost completely uncorrelated from those of individually tagged flavours.

9 Acknowledgement

This work has profited largely from the theoretical advice of G.Kramer, B.Lampe, L.Lönnblad, T.Sjöstrand and P.Zerwas. We gratefully acknowledge the many discussions and their helpful suggestions. We are particularly indebted to G.Kramer and B.Lampe and to L.Lönnblad for allowing us to use their calculation and the ARIADNE program before publication.

It is a pleasure to thank the SL Division for the efficient operation of the LEP accelerator, the precise information on the absolute energy, and their continuing close cooperation with our experimental group. In addition to the support staff at our own institutions we are pleased to acknowledge the following :
Department of Energy, USA
National Science Foundation, USA
Science and Engineering Research Council, UK
Natural Sciences and Engineering Research Council,Canada
Israeli Ministry of Science
Minerva Gesellschaft
The Japanese Ministry of Education, Science and Culture (the Monbusho) and a grant under the Monbusho International Science Research Program.
American Israeli Bi-national Science Foundation.
Direction des Sciences de la Matière du Commissariat à l'Energie Atomique, France.
The Bundesministerium für Forschung und Technologie, FRG.
and The A.P. Sloan Foundation.

References

[1] T.F.Walsh and P.Zerwas, Phys.Lett. *B44* (1973), 195; S.J.Brodsky, C.E.Carlson, and R.Suaya, Phys.Rev.*D14* (1976), 2264; K.Koller, T.F.Walsh, and P.Zerwas, Z.Physik *C2* (1979), 197

[2] P.Mättig and W.Zeuner, CERN-PPE 90-144 to be published in Z.Phys. C

[3] G.Kramer and B.Lampe, private communication

[4] T.Sjöstrand, Comp. Phys. Comm *39* (1986), 347; JETSET, Version 7.2

[5] L.Lönnblad, ARIADNE3.2 and private communication

[6] OPAL - Collaboration, M.Z.Akrawy et al., Phys.Lett. *B246* (1990) 285

[7] OPAL - Collaboration, K.Ahmet et al. CERN-PPE 90-114

[8] OPAL - Collaboration, M.Z.Akrawy et al., Phys.Lett *231B* (1989) 530; OPAL - Collaboration, G.Alexander et al., CERN-PPE/91-67

[9] JADE - Collaboration, W.Bartel et al., Z.Phys. *C33* (1986) 23; JADE - Collaboration, S.Bethke et al., Phys.Lett. *B123* (1988) 235

[10] OPAL - Collaboration, M.Z.Akrawy et al., Phys.Lett. *B253* (1991), 511;

[11] OPAL - Collaboration, M.Z.Akrawy et al., Phys. Lett. *241B* (1990) 133; OPAL - Collaboration, M.Z.Akrawy et al., Phys.Lett. *B257* (1991), 531;

[12] G.Marchesini and B.R.Webber, Nucl.Phys. *B310* (1988), 461; HERWIG, Version 3.2

[13] R.Brun et al., GEANT3 User's Guide, CERN DD/EE/84-1 (1989); J.Allison et al., Comp.Phys.Comm. *47* (1987) 55

[14] P.Mättig, Phys.Rep. *177* (1989) 141

[15] TPC - Collaboration, H.Aihara et al., Phys.Rev.Lett *61* (1988) 1263; TASSO - Collaboration, W.Braunschweig et al. Z.Phys *C42* 1989) 189

[16] F.A.Berends, R. Kleiss, S.Jadach, Nucl.Phys. *B202* (1982), 63

[17] OPAL - Collaboration, M.Z.Akrawy et al., Z.Phys. *C47* (1990) 505

[18] OPAL - Collaboration, G.Alexander et al., paper in preparation

[19] OPAL - Collaboration, M.Z.Akrawy et al., Z.Phys. *C49* (1991) 375

[20] G.Kramer and N.Magnusson, Z.Phys *C49* (1991) 301

[21] G.Kramer and B.Lampe, Fortschr. Phys. *37* (1989) 161

[22] ALEPH Collaboration, D.Decamp et al., Phys.Lett. *244B* (1990), 551

[23] OPAL Collaboration, M.Z.Akrawy et al., CERN-PPE/91-48

[24] DELPHI Collaboration, P.Abreu et al., CERN-PPE/90-123

[25] OPAL Collaboration, G.Alexander et al., CERN-PPE/91-63

[26] L3 Collaboration, B.Adeva et al., L3 Preprint 27-1991

10 Figure Captions

Figure 1: Comparison of cluster properties of candidate photons in multihadronic events (points with error bars) with those of photons of the reference sample of $e^+e^- \to \gamma\gamma$ and $l^+l^-\gamma$ (dotted area); (a) number of lead glass blocks per cluster (b) cluster width W in radians.

Figure 2: Cluster shape distribution of candidates in hadronic events (points with error bars), in the reference sample (dotted area), expected from the simulation of photons (thick curve) and expected from the simulation of π^0's (thin curve). The distributions are normalized to the number of photon candidates with C<1.5. (a) 7.5< E_γ <15 GeV, (b) 15< E_γ < 25 GeV, (c) E_γ > 25 GeV.

Figure 3: Observed fraction of multihadronic events with final state radiation of all multihadronic events as a function of y_{cut} and comparison to theoretical predictions (a) Matrix element calculation of Kramer and Lampe [3]. The shaded area indicates the theoretical uncertainty due to α_s. (b) Yields per 1000 multihadronic Z^0 decays for one, two and three jets and a photon. The bands show the expectation of the matrix element calculation [3]. (c) QCD shower models JETSET [4] (thick curve) and ARIADNE [5] (thin curve). In this case the assigned errors due to the energy and isolation cut are neglected.

Figure 4: (a) Correlation of couplings of up and down type quarks. Shown are the relations obtained within one standard deviation from the measured hadronic width and from the photon yield compared to the prediction of the matrix element calculation [3]. Also indicated is the standard model expectation. (b) Correlation plot Γ_u vs. Γ_d as obtained from this measurement. Displayed is the one standard deviation contour (narrow bar). Also shown are the partial widths of the Z^0 into charm and bottom quarks, combined from all LEP experiments. The standard model value is indicated.

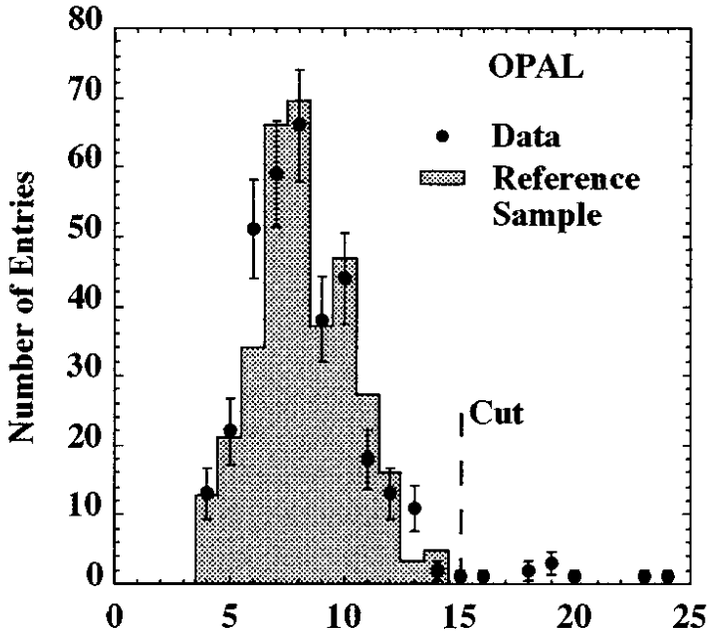

Figure 1a

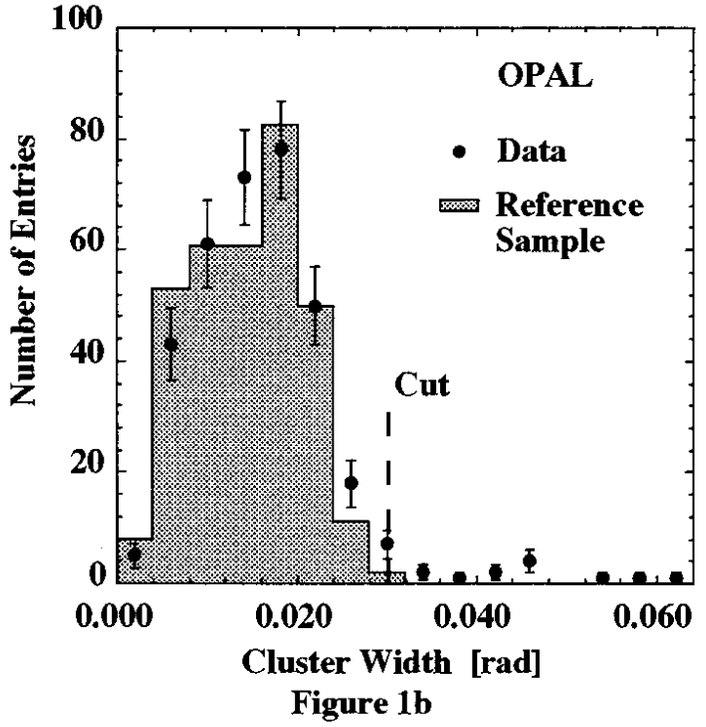

Figure 1b

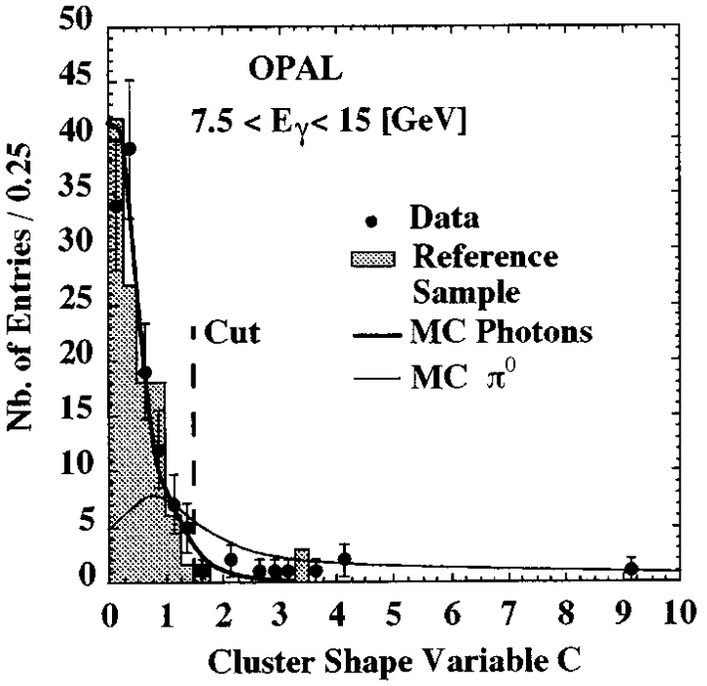

Figure 2a

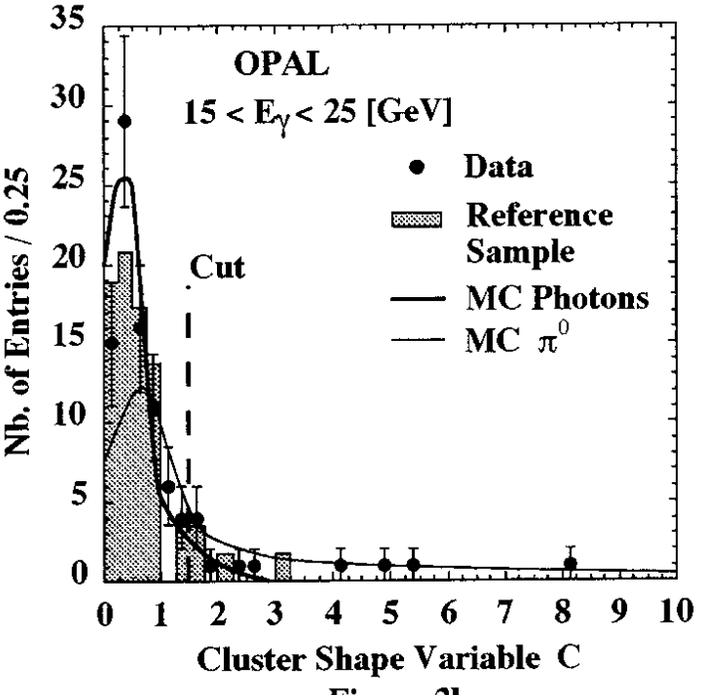

Figure 2b

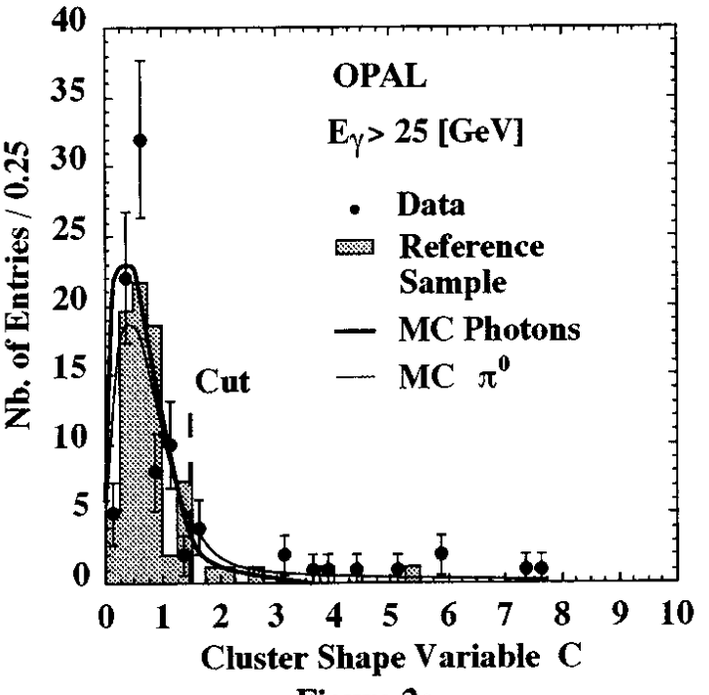

Figure 2c

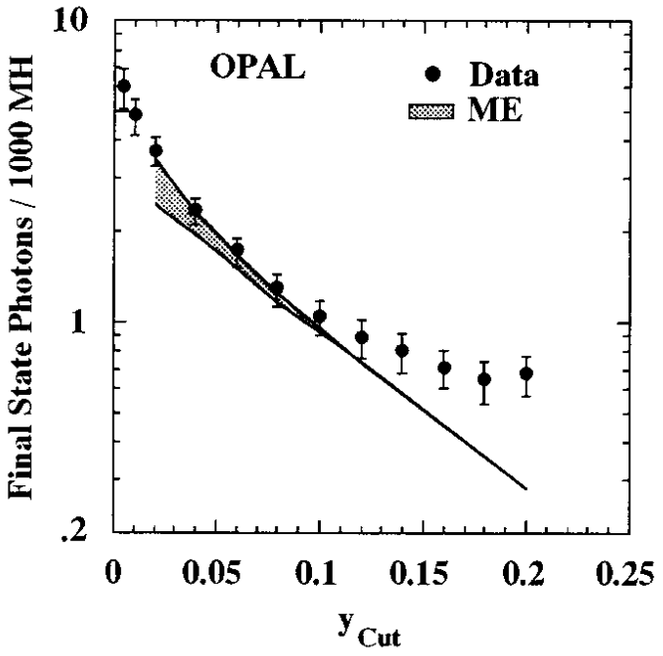

Figure 3a

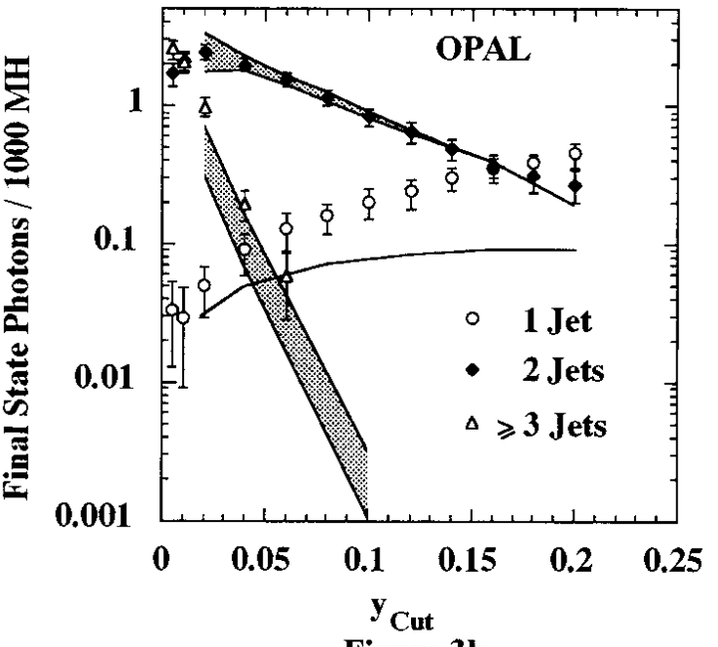

Figure 3b

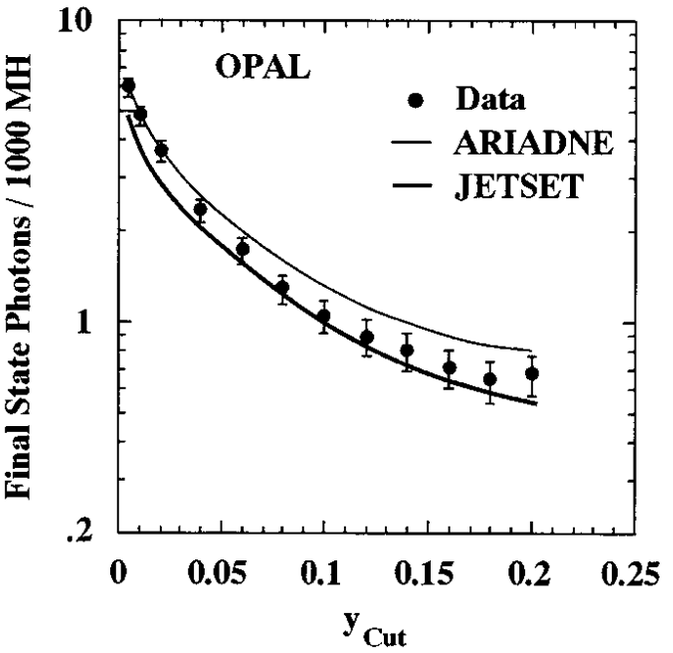

Figure 3c

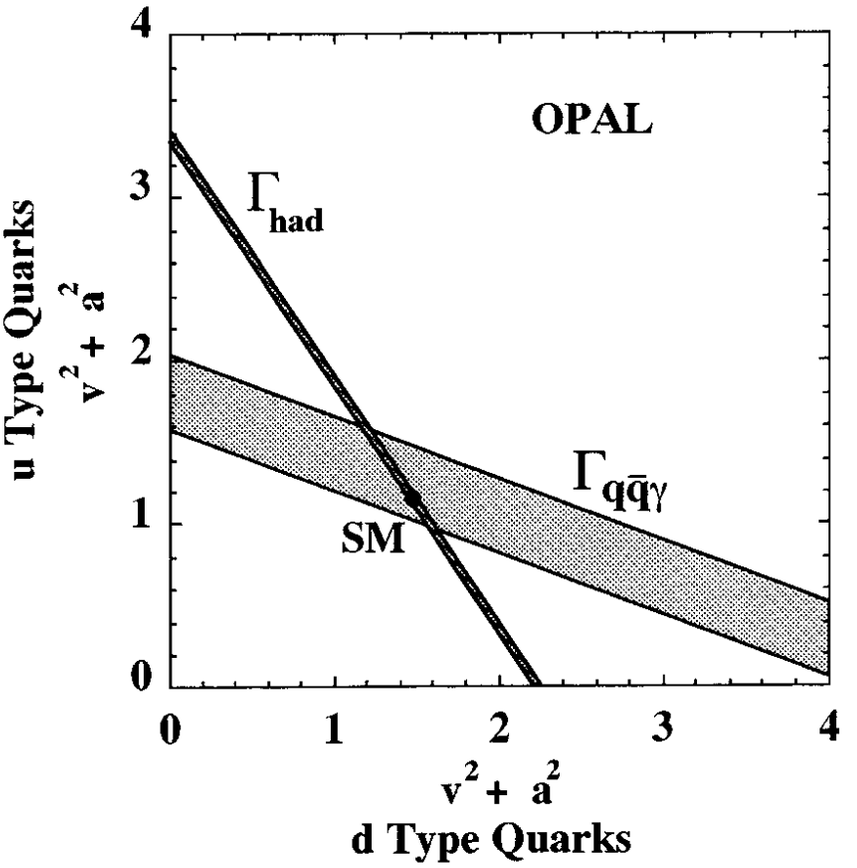

Figure 4 a

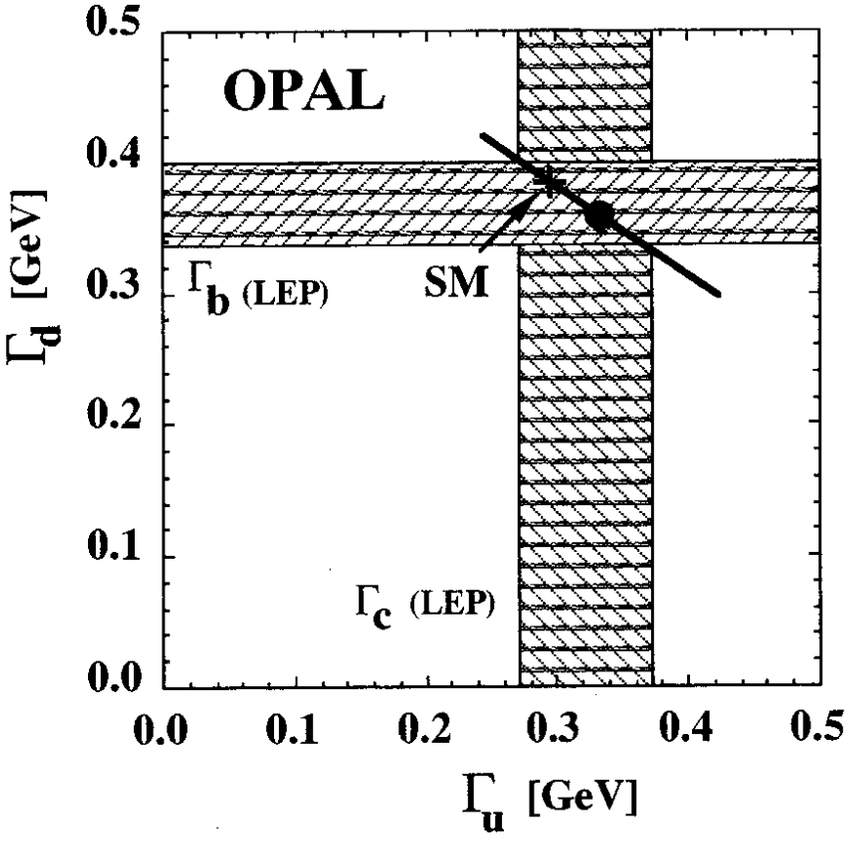

Figure 4b